Hindawi Publishing Corporation
Advances in Condensed Matter Physics
Volume 2014, Article ID 174362, 7 pages
http://dx.doi.org/10.1155/2014/174362

Research Article

Effect of Concurrent ZnO Addition and AlF_3 Reduction on the Elastic Properties of Tellurite Based Glass System

Haji Abdul Aziz Sidek,[1] Raouf El-Mallawany,[2] Krishnaswamy Hariharan,[3] and Shaharuddin Rosmawati[1]

[1] *Glass, Ceramic and Composite Research Group, Department of Physics, Faculty of Science, Universiti Putra Malaysia, 43400 Serdang, Selangor, Malaysia*
[2] *Department of Physics, Faculty of Science, Menofia University, Shebin Al-Kom, Egypt*
[3] *Department of Physics, Indian Institute of Technology Madras, Chennai, India*

Correspondence should be addressed to Haji Abdul Aziz Sidek; sidek@upm.edu.my

Received 30 April 2014; Revised 19 June 2014; Accepted 19 June 2014; Published 8 July 2014

Academic Editor: Changgui Lin

New ternary zinc oxyfluorotellurite (ZOFT) with the composition $(ZnO)_x$-$(AlF_3)_y$-$(TeO_2)_z$, where $5 \leq x < 35$; $5 \leq y \leq 25$; $60 \leq z \leq 70$, has been successfully prepared by the conventional rapid melt quenching technique. Density, molar volume, and glass transition temperature have been assessed for each ZOFT glass sample. The longitudinal and transverse ultrasonic waves propagated in each glass sample were measured using a MBS8020 ultrasonic data acquisition system at 5 MHz frequency and room temperature. The longitudinal modulus (L), shear modulus (G), Young's modulus (E), bulk modulus (K), and Poisson's ratio (σ) are assessed from both velocity data and their respective density. The compositional dependence of the ultrasonic velocities and related parameters are discussed to understand the rigidity and compactness of the glass system studied.

1. Introduction

Tellurite glasses are very interesting glasses due to their unique physical properties and applications [1–12]. Tellurite glass was applied at the back of amorphous silicon solar cells in combination with a rear reflector to improve the efficiency of the cell [3]. The propagation of ultrasonic waves in solids provides valuable information about the solid state motion in the material. In recent years, the subject of glasses has rapidly increased because of their various applications in electronics, nuclear and solar energy technologies, and acoustooptic devices [11, 12]. The acoustic wave propagation in bulk glasses has been of considerable interest to understand their mechanical properties. Elastic properties provide information on the structures of solids which are directly related to the interatomic potentials. Glasses are isotropic and have only two independent elastic constant: longitudinal and shear elastic moduli. These two parameters are obtained from the longitudinal and shear sound velocities and density of the glass [13]. An extensive series of research works related to elastic properties of binary, ternary, and quaternary tellurite glasses have been carried out recently [14–23].

The choice of new ternary glass series, namely, zinc oxyfluorotellurite (ZOFT), is of particular interest since they are expected to have chemical durability and thermal stability representing a compromise between pure fluoride and oxide glass with flexible optical properties. Furthermore, the introduction of metal halides into the system could improve such properties and will decrease their hygroscopic behaviour which limits the applications of many pure halides glasses. Also, the main objective of the current work is to study the effect of concurrent ZnO addition and AlF_3 reduction on the density and the elastic properties of zinc tellurite glass systems.

2. Materials and Experimental Method

Zinc oxyfluorotellurite (ZOFT) with the composition $(ZnO)_x$-$(AlF_3)_y$-$(TeO_2)_z$, where $5 \leq x < 35$; $5 \leq y \leq 25$;

Table 1: Starting composition bulk density, molar volume, glass transition temperature (T_g), and molecular weight of ZOFT $(ZnO)_x(AlF_3)_y(TeO_2)_z$ glass systems at room temperature.

Sample Code	Glass Composition (mol%)			Density ($g\,cm^{-3}$)	Molar Volume ($10^{-6}\,cm^{-3}$)	T_g (°C)
	ZnO	AlF_3	TeO_2			
P1	5	25	70	4.67	29.28	391
P2	10	20	70	4.84	28.24	387
P3	15	15	70	4.91	27.83	386
P4	20	10	70	5.01	27.24	383
P5	25	5	70	5.13	26.54	374
Q1	10	25	65	4.7	28.25	395
Q2	15	20	65	4.86	27.34	390
Q3	20	15	65	4.97	26.69	384
Q4	25	10	65	5.04	26.3	380
Q5	30	5	65	5.14	25.76	373
R1	15	25	60	4.72	27.32	397
R2	20	20	60	4.96	26.02	384
R3	25	15	60	5.07	25.04	376
R4	30	10	60	5.11	25.14	371
R5	35	5	60	5.19	24.77	362

$60 \le z \le 70$, has been successfully synthesized using the rapid melt quenching method and x, y, z are mole % as shown in Table 1. Detailed preparation of these types of glasses is well documented and available elsewhere [14–17]. The density (ρ) of the glasses was determined by the Archimedes method with acetone as floating liquid. All the glass samples' weight was measured with a digital balance (±0.0001 g accuracy). Their molar volume was calculated from the molecular weight (M) and density (ρ). The accuracy in the measurement of the density is $\pm 0.01\,g\,cm^{-3}$ and the relative error is ±0.05%. All the glass samples were checked by X-ray diffraction for their amorphous nature using X'Pert Pro Panalytical PW 3040 MPD X-ray powder diffractometer by employing Cr-Kα radiation. The glass transition temperature (T_g) was determined by the differential thermogravimetric analysis (SETARAM instrumentation Labsys DTA/6) at a heating rate of 20 K min^{-1}. The accuracy in the measurement of (T_g) is ±2°C.

Ultrasonic velocity measurements were carried out at a frequency of 10 MHz using x-cut and y-cut quartz transducers. A pulse superposition technique was employed using Ultrasonic Data Acquisition System (MATEC 8020, Matec Instruments, USA) [17, 18]. Burnt honey was used as a bonding material between the glass samples and transducers. By measuring the thickness of the sample (d), longitudinal (V_l), and transverse (V_t), wave velocities were calculated using the relation $V = 2d/t$. The absolute accuracy in the measurement of the velocity is $\pm 5\,m\,s^{-1}$ and the relative error is ±0.1%. The detailed information related with the experimental method has been discussed elsewhere [20–22].

Glasses are isotropic and have only two independent elastic constants of L and G which can be obtained from their longitudinal and shear sound wave velocity and density. The various elastic properties of the glasses were calculated using the following standard relations [13, 21]:

$$\begin{aligned}
&\text{Longitudinal modulus } L = \rho V_1^2,\\
&\text{Shear modulus } G = \rho V_s^2,\\
&\text{Bulk modulus } K = \rho\left(V_l^2 - \frac{4}{3}V_s{}^2\right),\\
&\text{Young's modulus } E = \frac{\rho V_s^2\left(3V_l^2 - 4V_s^2\right)}{V_l^2 - V_s^2},\\
&\text{Poisson's ratio } \sigma = \frac{\left(V_l^2 - 2V_s^2\right)}{2\left(V_l^2 - V_s^2\right)},\\
&\text{Fractal dimensionality } d = \frac{4G}{K}.
\end{aligned} \tag{1}$$

3. Results and Discussion

3.1. Glass Composition. Table 1 shows the composition of glass series of zinc oxyfluorotellurite (ZOFT) which have an empirical formula of $(ZnO)_x$-$(AlF_3)_y$-$(TeO_2)_z$, where $5 \le x < 35$; $5 \le y \le 25$; $60 \le z \le 70$, where their densities, molar volumes, and glass transition temperature (T_g) are also included. Three systematic series of ZOFT glass system each denoted with Pn, Qn, and Rn ($n = 1, \ldots, 5$) have been successfully prepared. It was observed that the color of glass sample changes from semitransparent yellow to transparent yellow as more AlF_3 content is added to the ZOFT glass system as shown in Figure 1.

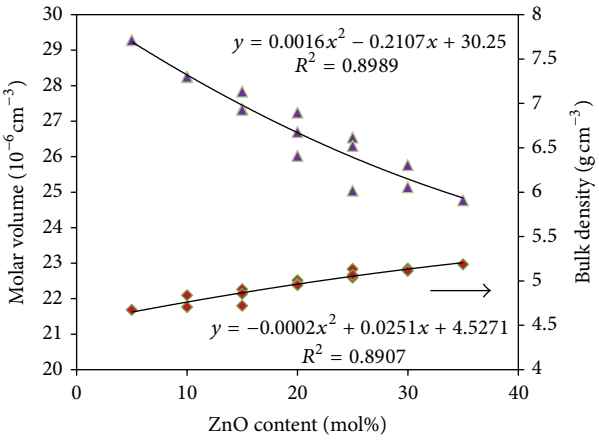

FIGURE 1: The variation of density and molar volume of ZOFT glass series at various ZnO contents (mol%).

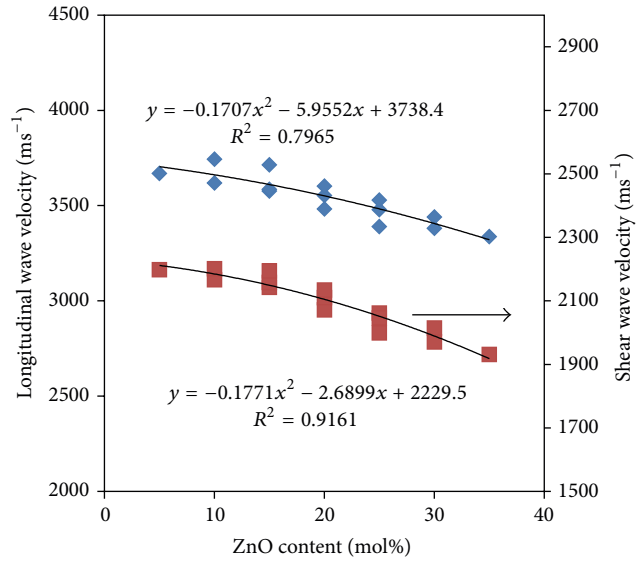

FIGURE 2: Variation of longitudinal, v_l (top), and shear, v_s (bottom), ultrasonic wave velocities for ZOFT glass series.

3.2. Density. As shown in Figure 1 and Table 1, the densities of all ZOFT glass series increase as the ZnO was added to substitute the AlF_3 content in the tellurite based glass network system where the trend shows the similar pattern as in the binary zinc tellurite [14, 17]. Generally, the variation of density of ZOFT glass is in accord with their molecular weight where the molecular weight of the glass series increases as more AlF_3 content is substituted by ZnO in the tellurite glass network. However, the existence of AlF_3 in zinc tellurite glass causes the values of the densities to be slightly lower than that of binary ZnO-TeO_2 glass samples which range from 4.80 to 5.28 cm^{-3} [17]. The present results are in good agreement with the earlier statement of Mallawany's that the halogen substitution lowered the density of the glass sample [11, 13]. Even the addition of $ZnCl_2$ into the oxychloride glass system (TeO_2-ZnO-$ZnCl_2$) also lowered the densities of the TeO_2-ZnO glass system [24, 25]. Density values of (50-x)ZnO-$x$$Bi_2O_3-50V_2O_5$ [26] were changed from 3.5 to 5.13 g/cm^3.

As shown in Figure 1, the densities increase linearly with the concurrent addition of ZnO and reduction of AlF_3 content. In this case, as more ZnO content is added into the zinc tellurite glass system, two Zn–F single bonds will replace the Zn=O double bonds; hence, the structure of the glasses becomes close-packed, which results in an increase in density. Fluorine plays an important role in the glass matrix; replacing the O^{2-} ions causes the compositional dependence of the density and molar volume [27]. The molecular weight of TeO_2 is 159.599 which is greater than AlF_3 (83.977) and ZnO (81.408), whereas the atomic weight of individual constituent atom is Te (127.6) > Zn (65.39) > Al (26.9815) > F (18.998) > O (15.9999) and the atomic radius of each of the constituent atoms (in ppm) is Al (143) > Te (140) > Zn (134) > O (66) > F (64).

3.3. Molar Volume. Figure 2 also shows the variation of molar volume with ZnO content for all ZOFT glass series. The decrease in molar volumes for all glass systems which range from 29.28 to 24.77 × 10^{-6} cm^3/mol attributed to a decrease in the bond length or interatomic spacing between the atoms. The radius of Te^{2+} (0.097 nm) is much greater than that of Zn^{2+} (0.074 nm) and since the radius of Al^{3+} is 0.0535 nm which also has a smaller radius than Zn^{2+} attributed to this situation. Molar volume of the pure TeO_2 glass was 31.28 × 10^{-6} cm^3/mol [13]. The current finding shows that the molar volume for ZOFT glass system results shows slightly higher values than that of the binary zinc tellurite glasses [14]. The much higher reduction in the molar volume for the ZOFT glass sample containing flourine is attributed to the decrease in viscosity due to the breaking of the Te–O–Te bond to form two Te–F bonds, which increase the efficiency of the crystallization process [28]. The addition of ZnO that consists of Zn^{2+} will certainly modify the tellurite glass structure by creating NBOs in the network, and this situation might occur in ZOFT glass system. The NBOs created were believed to alter the glass structure in a way that packing of the molecule becomes denser as more network modifier ions (in this case Al^{3+}) attempt to occupy the interstices within the network.

3.4. Glass Transition. In the present investigation, all of the glasses have an endothermic change between 362 and 395°C which attributes to the glass transition temperature, T_g. The Zn^{2+} is incorporated into the glass structure as a network modifier, resulting in closed packing of the glass structure. However, a continuous decrease in T_g with the increase in network modifier contents of ZnO and reduction of AlF_3 has been observed as collected in Table 1. In the present glasses, the decrease in T_g values with increase in Zn^{2+} content contributes to a decrease in thermal stability of the ZOFT glasses that will be discussed elsewhere. The glass transition reflects a change in the coordination number of the network forming atoms and destruction of the network structure brought about by the formation of some nonbridging atoms. The decrease in the glass transition temperature values implies that the number of bridging oxygen groups

Table 2: The longitudinal and shear ultrasonic velocities and their ratio for ZOFT glass series.

Sample code	Ultrasonic wave velocity ($m\,s^{-1}$)		V_l/V_s
	V_l	V_s	
P1	3669	2198	1.67
P2	3618	2166	1.67
P3	3576	2142	1.67
P4	3482	2071	1.68
P5	3390	1999	1.70
Q1	3743	2201	1.70
Q2	3585	2158	1.66
Q3	3553	2110	1.68
Q4	3478	2061	1.69
Q5	3380	1970	1.72
R1	3714	2194	1.69
R2	3601	2134	1.69
R3	3528	2046	1.72
R4	3440	2014	1.71
R5	3337	1931	1.73

decreases. This is mainly due to the addition of ZnO which weakens the bond between each atom (increases the number of NBOs atom). The bond is easier to break and hence the T_g of the sample decreased. Furthermore, it also implies a decrease in rigidity of the glass network. It was observed that replacing O^{2-} with F^- in the oxyfluoride tellurite glass matrix causes the compositional dependence of the glass transition temperature, T_g, and other physical properties in the ZOFT glass system.

3.5. Sound Wave Velocity. Figure 2 depicts the variation of longitudinal and shear velocities for ZOFT glass series. The variation of both wave velocities that propagated in the present ZOFT bulk glass samples strongly depends on the structural change of the glass network. The longitudinal and shear ultrasonic velocities for each ZOFT glass series are given in Table 2 for a different mole fraction of ZnO content. As shown in Figure 2, it can be seen that, in the glasses studied, both longitudinal and shear ultrasonic velocities decrease nonlinearly with ZnO addition to substitute the AlF_3 in the ZOFT glass system for all series.

It is obviously seen that the decreasing values of both velocities are much higher (>10%) in the lower concentration of 60 mol% TeO_2 as compared with 70 mol% TeO_2 glass series (>7%). For instance, the longitudinal velocity for R1 to R5 (TeO_2 : 0.60) glass samples decreases from 3714 m/s to 3337 m/s and shear velocity from 2194 m/s to 1931 m/s as the ZnO content increases from 15 to 35 mol% and AlF_3 content decreases from 25 to 5 mol%, whereas the longitudinal velocity for P glass series (TeO_2 : 70) glass samples decreases from 3669 m/s to 3390 m/s as the ZnO content increases from 5to 25 mol% and AlF_3 content decreases from 25 to 5 mol%. The overall percentage decrease of velocities of each glass series is given in Table 3. It is noticed that the percentage of decrement in velocity increases with the increasing of substituting AlF_3 content. It means that the more AlF_3 substitution to ZnO content, the higher the difference between maximum velocity and minimum velocity for both longitudinal and shear velocity. The observed difference between higher values at low TeO_2 content ($x = 60$ mol%) and lower values at high TeO_2 content ($x = 70$ mol%) in the velocity confirms a substantial change in the glass structure. The decrease in AlF_3 content decreases velocities through glass, and elastic stiffness is also reduced as observed earlier [25]. As small quantity of AlF_3 is added into the TeO_2-ZnO glass network, a breaking of Te–O–Te takes place. The conversion of this linkage results in depolymerization of network leading to the formation of $Te-_{ax}O_{eq}-Te$ bridges with the apparition of nonbridging oxygen (NBO) [29]. Therefore, the continual breaking of the Te–O–Te linkages with addition of ZnO to substitute AlF_3 contents leads to the loose packing of the glass network and, hence, a decrease in rigidity. The observed results can be further substantiated by revealing the composition dependent ultrasonic parameters.

It is inferred that a decrease in Te coordination number (N) has resulted with the increase in the modifier content [30]. Further, a decrease in the coordination number results in slight decrease in the mean Te-O bond length (R) [29]. Thus, it is inferred that the observed continuous decrease in sound velocity in the present glasses is due to the change in coordination number with the addition of ZnO to substitute AlF_3content. An introduction of fluorine into TeO_2-based glass system results in reduction of Te-O-Te linkages due to a gradual transformation of trigonal bipyramid TeO_4 (tbp) through TeO_{3+1} to trigonal pyramid TeO_3 decreasing the connectivity of the tellurite glass former network. This behaviour is strengthened by the higher concentration of F^- ions [27].

3.6. Elastic Moduli. Elastic modulus of the present ZOFT glass series has been determined from the measured ultrasonic velocities and densities. Table 4 presents the experimental values of the elastic moduli: Young's modulus (E), longitudinal modulus (L), shear modulus (G), bulk modulus (K), and Poisson's ratio (σ) for each ZOFT glass series.

For P1 to P5 glass series, Young's modulus decreases from 32.80 to 31.64 GPa. This pattern is applied to the rest of ZOFT glass series. The addition of ZnO and AlF_3 reduction result in low network rigidity, which in turn results in decrease of the longitudinal (L) and shear (G) modulus. The decrease of shear modulus (G) and bulk modulus (K) is probably due to the tendency of the change in the coordination number of Te in the ZOFT glass network. For the ZOFT glasses both the degree of cross-linking and the relative proportions of different types of bonds may be changed with the glass composition. The existence of AlF_3 and the nature of TeO_2 not only cause a decrease in the elastic moduli, but also cause an increase in Poisson's ratio (Table 4).

3.7. Poisson's Ratio. It has been reported that Poisson's ratio is affected by the changes in the cross-link density of the glass network. The glass structure with high cross-link density has

Table 3: Variation of ultrasonic velocities due to ZnO addition and AlF_3 reduction in the tellurite glass network.

Sample code	Longitudinal velocity (m/s)		Percent of decrease in velocity (%)	Shear velocity (m/s)		Percent of decrease in velocity (%)
	Maximum	Minimum		Maximum	Minimum	
P1–P5	3669	3390	7.60	2198	1999	9.05
Q1–Q5	3743	3380	9.70	2201	1970	10.49
R1–R5	3714	3337	10.15	2194	1931	11.99

Table 4: Longitudinal (L), shear (G), Young's (E), and bulk (K) modulus, Poisson's ratio (σ), and fractal bond connectivity (d) for ZOFT glass series.

Sample code	Elastic moduli (GPa)				σ	$d = 4G/K$
	L	G	K	E		
P1	62.89	22.57	32.80	55.08	0.220	2.753
P2	63.33	22.70	33.07	55.41	0.221	2.746
P3	62.72	22.50	32.72	54.92	0.220	2.751
P4	60.71	21.48	32.07	52.67	0.226	2.678
P5	58.99	20.51	31.64	50.60	0.233	2.593
Q1	65.90	22.79	35.52	56.32	0.236	2.566
Q2	62.40	22.61	32.25	54.98	0.216	2.804
Q3	62.73	22.12	33.23	54.31	0.228	2.663
Q4	60.93	21.40	32.40	52.61	0.229	2.641
Q5	58.70	19.94	32.11	49.56	0.243	2.484
R1	65.11	22.72	34.81	55.98	0.232	2.613
R2	64.21	22.55	34.15	55.45	0.229	2.642
R3	63.06	21.21	34.78	52.87	0.247	2.439
R4	60.51	20.74	32.85	51.40	0.239	2.525
R5	57.75	19.34	31.97	48.28	0.248	2.420

Poisson's ratio in the order of 0.1 to 0.2, while structure with low cross-link density has Poisson's ratio in the order of 0.3 to 0.5. As shown in Figure 4, Poisson's ratio of the present glass shows a nonlinear increase as the ZnO content increases for all glass series. For instance, from Q1 to Q5 glass series, Poisson's ratio increases from 0.232 to 0.248. Hence the values of the Poisson's ratio are of the order 0.2 which reveals a high cross-link density [29]. Poisson's ratio obtained from the calculation shows reverse changes and trend compared to other elastic moduli. The variation of Poisson's ratio with composition should be exactly the reverse of elastic moduli variation [31]. For all series of glass, the transformation of cross-linkage is negligibly small (changes about 0.02) and almost remains constant. Flourine plays a role in decreasing the connectivity of the glass structure. It also indicates a strengthening in the glass structure which may be due to the introduction of stronger ionic bonds in the glass network [31, 32].

3.8. Fractal Bond Connectivity. The fractal bond connectivity (d) is a ratio between shear to bulk modulus ratio ($4G/K$)of ZOFT glass series at room temperature and is presented in Table 4. The fractal bond connected as shown in Figure 4 for ZOFT glass series tends to decrease with increasing ZnO content which is consistent with the loss or weakening of cross-link between TeO_2 chains. In this study, the fractal bond connectivity, (d), of these glasses ranges between 2.804 and 2.420. These suggest an intermediate connectivity between a two- and a three-dimensional disordered network, which implies a marked degree of cross-linkage between TeO_2 chains, as would be anticipated for modifier cations whose valence is greater than unity, or increased branching of the network of TeO_2 chains facilitated by an increase in the number of endings and branching units incorporated into the basic tellurite network.

3.9. Regression Analysis. All the current experimental data obtained from ZOFT glass series were analyzed using Microsoft Excel, with nonlinear fitting regression curves, where the results of the regression coefficients are presented in Table 5. The regression coefficients obtained from each curve are shown in Figures 1, 2, 3, and 4. In Table 5, Y stands for the variables shown in the first column. As can be seen in previous figures, for most of the variables, a nonlinear curve ($Y = Ax^2 + Bx + C$) gives the best fit. Except for Young's modulus (E), the R^2 values lie between 0.622 and 0.9161.

4. Conclusion

New ternary zinc oxyfluorotellurite (ZOFT) with the compositions $(ZnO)_x$-$(AlF_3)_y(TeO2)_z$, where $5 \leq x < 35$; $5 \leq y \leq 25$; $60 \leq z \leq 70$, has been achieved. The characteristics of

Table 5: Nonlinear regression analysis of the variables ($y = Ax^2 + Bx + C$) for various properties of ZOFT glass series.

Variable	A	B	C	R^2
Density	−0.163	25.09	4527.1	0.8907
Molar Volume	0.002	−0.211	30.25	0.8989
Longitudinal wave velocity (V_l)	−0.171	−5.955	3738.4	0.7965
Shear wave velocity (V_s)	−0.177	−2.690	2229.5	0.9161
Longitudinal modulus (L)	−0.009	0.132	63.4	0.6626
Shear modulus (G)	−0.005	0.063	22.56	0.906
Bulk modulus (K)	−0.010	0.144	55.18	0.870
Poisson's ratio (sigma)	3×10^{-5}	−0.0004	0.224	0.623
Fractal Bond connectivity	−0.0004	0.0044	2.707	0.622
Glass temperature, T_g	−0.033	0.298	664.74	0.886

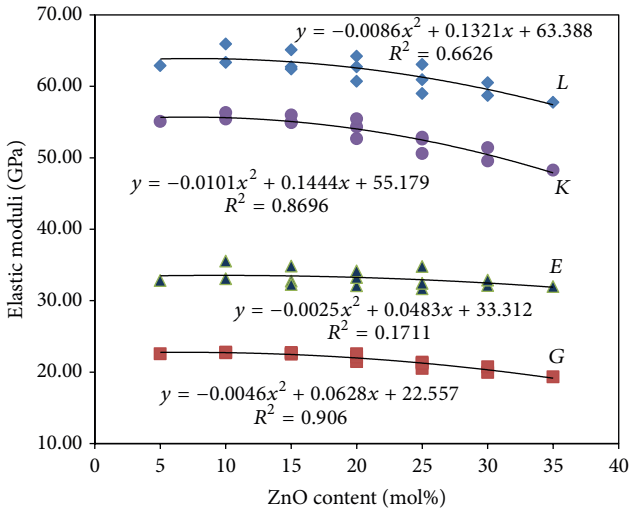

Figure 3: Variation of elastic moduli (i.e., longitudinal modulus (L), shear modulus (G), bulk modulus (K), and Young's modulus (E) for ZOFT glass series).

ZOFT glass series were studied with the effect of concurrent ZnO addition and AlF_3 reduction in the tellurite glass matrix.

(i) The densities of the ZOFT glasses increase as the ZnO content was added to substitute the AlF_3 content for ZOFT glass series while their molar volume decreases. The increase in density was due to the decrease of molar volume as well as interatomic spacing.

(ii) The glass transition temperatures show the decreasing trend with the addition of ZnO content. These decreases can be explained by the role of the fluorine ions which substitute the TeO_2-ZnO network.

(iii) The observed decrease in ultrasonic velocities confirmed a substantial change in the glass structure. The concurrent Zn addition and AlF_3 reduction in the tellurite glass matrix cause more ions to be opened up in the network. Thus, weakening of the glass structure or reduction in the rigidity of the network takes place.

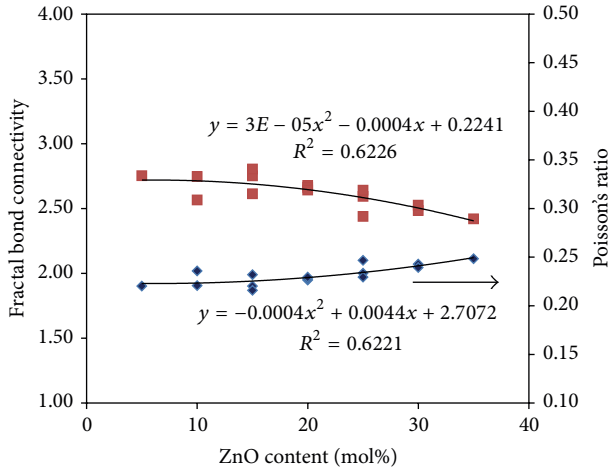

Figure 4: Variation of Poisson's ratio and fractal bond connectivity of ZOT glass series at various ZnO contents.

(iv) All elastic constants decrease with the addition of the ZnO content and AlF_3 reduction in the ZOFT glass series. The effect of the halogen substitution F^- on the elastic properties was expected to produce quite different changes in physical properties.

Conflict of Interests

The authors declare that there is no conflict of interests regarding the publication of this paper.

Acknowledgments

The financial support from Ministry of Science, Technology and Innovation, Malaysia, and Universiti Putra Malaysia (UPM), each under the Fundamental Research Grant Scheme (vote no. 5524288) and Research University Grant Scheme (vote no. 9340800), is gratefully acknowledged.

References

[1] T. Cheng, K. Asano, Z. Duan et al., "Design and optimization of tellurite hybrid microstructured optical fiber with high nonlinearity and low flattened chromatic dispersion for optical parametric amplification," *Optics Communications*, vol. 318, pp. 105–111, 2014.

[2] R. N. Hampton, W. Hong, G. A. Saunders, and R. A. El-Mallawany, "The dielectric properties of tellurite glass," *Physics and Chemistry of Glasses*, vol. 29, no. 3, pp. 100–105, 1988.

[3] F. Yang, C. Liu, D. Wei, Y. Chen, J. Lu, and Sh. Yang, "Er^{3+}-Yb^{3+} co-doped TeO_2-PbF_2 oxyhalide tellurite glasses for amorphous silicon solar cells," *Optical Materials*, vol. 36, pp. 1040–1043, 2014.

[4] R. A. El-Mallawany, L. M. Sharaf El-Deen, and M. M. Elkholy, "Dielectric properties and polarizability of molybdenum tellurite glasses," *Journal of Materials Science*, vol. 31, no. 23, pp. 6339–6343, 1996.

[5] I. Z. Hager, R. El-Mallawany, and M. Poulain, "Infrared and Raman spectra of new molybdenum and tungsten oxyfluoride

glasses," *Journal of Materials Science*, vol. 34, no. 21, pp. 5163–5168, 1999.

[6] R. El-Mallawany, "Quantitative analysis of elastic moduli of tellurite glasses," *Journal of Materials Research*, vol. 5, no. 10, pp. 2218–2222, 1990.

[7] S. Laila, A. Suraya, and A. Yahya, "Effect of glass network modification on elastic and structural properties of mixed electronic-ionic $35V_2O_5$-(65-x)TeO_2-(x)Li_2O glass system," *Chalcogenide Letters*, vol. 11, pp. 91–104, 2014.

[8] H. M. M. Moawad, H. Jain, and R. El-Mallawany, "DC conductivity of silver vanadium tellurite glasses," *Journal of Physics and Chemistry of Solids*, vol. 70, no. 1, pp. 224–233, 2009.

[9] R. El-Mallawany, A. Abousehly, and E. Yousef, "Elastic moduli of tricomponent tellurite glasses TeO_2-V_2O_5-Ag_2O," *Journal of Materials Science Letters*, vol. 19, no. 5, pp. 409–411, 2000.

[10] F. Nawaz, M. R. Sahar, S. K. Ghoshal, A. Awang, and I. Ahmed, "Concentration dependent structural and spectroscopic properties of $Sm3^+$ /$Yb3^+$ co-doped sodium tellurite glass," *Physica B: Condensed Matter*, vol. 433, pp. 89–95, 2014.

[11] R. El-Mallawany and I. A. Ahmed, "Thermal properties of multicomponent tellurite glass," *Journal of Materials Science*, vol. 43, no. 15, pp. 5131–5138, 2008.

[12] R. El-Mallawany, A. Abousehly, A. A. El-Rahamani, and E. Yousef, "Radiation effect on the ultrasonic attenuation and internal friction of tellurite glasses," *Materials Chemistry and Physics*, vol. 52, no. 2, pp. 161–165, 1998.

[13] R. El-Mallawany, "Tellurite glasses part 1. Elastic properties," *Materials Chemistry and Physics*, vol. 53, no. 2, pp. 93–120, 1998.

[14] H. A. A. Sidek, S. Rosmawati, Z. A. Talib, M. K. Halimah, and W. M. Daud, "Synthesis and optical properties of ZnO-TeO_2 glass system," *American Journal of Applied Sciences*, vol. 6, no. 8, pp. 1489–1494, 2009.

[15] S. Rosmawati, H. A. A. Sidek, A. T. Zainal, and H. Mohd Zobir, "IR and UV spectral studies of zinc tellurite glasses," *Journal of Applied Sciences*, vol. 7, no. 20, pp. 3051–3056, 2007.

[16] P. Gayathri Pavani, K. Sadhana, and V. Chandra Mouli, "Optical, physical and structural studies of boro-zinc tellurite glasses," *Physica B: Condensed Matter*, vol. 406, no. 6-7, pp. 1242–1247, 2011.

[17] H. A. A. Sidek, S. Rosmawati, M. K. Halimah, K. A. Matori, and Z. A. Talib, "Effect of AlF_3 on the density and elastic properties of zinc tellurite glass systems," *Materials*, vol. 5, no. 8, pp. 1361–1372, 2012.

[18] S. Rosmawati, H. A. A. Sidek, A. T. Zainal, and H. M. Zobir, "Effect of zinc on the physical properties of tellurite glass," *Journal of Applied Sciences*, vol. 8, no. 10, pp. 1956–1961, 2008.

[19] J. N. Ayuni, M. K. Halimah, Z. A. Talib et al., "Optical properties of ternary TeO_2-B_2O_3-ZnO glass system," *IOP Conference Series: Materials Science and Engineering*, vol. 17, no. 1, Article ID 012027, 2011.

[20] M. K. Halimah, W. M. Daud, and H. A. A. Sidek, "Elastic properties of TeO_2-B_2O_3-Ag_2O glasses," *Ionics*, vol. 16, no. 9, pp. 807–813, 2010.

[21] S. H. Ab Aziz, R. Sharuddin, K. A. Matori, and H. M. Kamari, "Elastic moduli of zinc oxyfluorotellurite glasses," *Journal of Materials Science and Engineering*, vol. 5, no. 3, pp. 319–322, 2011.

[22] H. A. A. Sidek, S. Rosmawati, K. A. Matori, M. K. Halimah, and B. Z. Azmi, "Elastic constants of $(TeO_2)_{90}(Alf_3)_{10-x}(ZnO)_x$ zinc oxyfluorotellurite glasses," *IOP Conference Series: Materials Science and Engineering*, vol. 17, no. 1, Article ID 012031, 2011.

[23] H. A. A. Sidek, S. Rosmawati, B. Z. Azmi, and A. H. Shaari, "Effect of ZnO on the thermal properties of tellurite glass," *Advances in Condensed Matter Physics*, vol. 2013, Article ID 783207, 6 pages, 2013.

[24] M. R. Sahar and N. Noordin, "Oxychloride glasses based on the TeO_2-ZnO-$ZnCl_2$ system," *Journal of Non-Crystalline Solids*, vol. 184, no. 1, pp. 137–140, 1995.

[25] R. A. El-Mallawany and G. A. Saunders, "Elastic behaviour under pressure of the binary tellurite glasses TeO_2-$ZnCl_2$ and TeO_2-WO_3," *Journal of Materials Science Letters*, vol. 6, no. 4, pp. 443–446, 1987.

[26] R. Punia, R. Kundu, J. Hooda, S. Dhankhar, S. Dahiya, and N. kishore, "Effect of Bi_2O_3 on structural, optical, and other physical properties of semiconducting zinc vanadate glasses," *Journal of Applied Physics*, vol. 110, Article ID 033527, 2011.

[27] G. Wang, S. Dai, J. Zhang, S. Xu, L. Hu, and Z. Jiang, "Effect of F- ions on physical and spectroscopic properties of Yb3+-doped TeO_2-based glasses," *Journal of Luminescence*, vol. 113, no. 1-2, pp. 27–32, 2005.

[28] S. Likitvanichkul and W. C. Lacourse, "Effect of fluorine content on crystallization of canasite glass-ceramics," *Journal of Materials Science*, vol. 30, no. 24, pp. 6151–6155, 1995.

[29] A. N. Begum and V. Rajendran, "Structure and elastic properties of TeO_2-BaF_2 glasses," *Journal of Physics and Chemistry of Solids*, vol. 67, no. 8, pp. 1697–1702, 2006.

[30] A. Ibanez, T. Ericsson, O. Lindqvist, D. Bazin, and E. Philippot, "Local range order of tellurium atoms in TeO_2-BaO and TeO_2-BaF_2 glassy systems," *Journal of Materials Chemistry*, vol. 4, no. 7, pp. 1101–1106, 1994.

[31] A. El-Adawy and Y. Moustafa, "Elastic properties of bismuth borate glasses," *Journal of Physics D: Applied Physics*, vol. 32, no. 21, pp. 2791–2796, 1999.

[32] R. El-Mallawany, M. Sidkey, A. Khafagy, and H. Afifi, "Ultrasonic attenuation of tellurite glasses," *Materials Chemistry and Physics*, vol. 37, no. 2, pp. 197–200, 1994.